CIMAC CONGRESS 25
ZURICH, MAY 19 – 23, 2025

2025 | 100

Virtualization of Fuel Injection System Development for Methanol-Fueled Large-Bore Marine Engines

Simulation Technologies, Digital Twins and Complex System Simulation

Ugo OLIVAUD, GammaTech Engineering

Erwann Le Callonnec, GammaTech Engineering
Alessio Desenibus, Wärtsilä
Irene Gallici, Wärtsilä
Francesco Mosca, Wärtsilä
Francesco Pasotti, Wärtsilä
Luca Zuanigh, Wärtsilä

ABSTRACT

Methanol has garnered significant attention as an alternative fuel in internal combustion engines, particularly for naval applications, due to its potential as a pathway towards carbon-neutral or even carbon-negative marine operations. However, the adoption of methanol in ICEs faces several challenges, especially in the design of the fuel injection circuit, due to issues such as its corrosiveness, toxicity, and low lubricity. In this context, numerical simulation, particularly 1D multi-physics modeling with GT-SUITE, is seen as a key enabler to accelerate the time to market and simultaneously reduce costs by minimizing the need for extensive prototyping and experimental measurements.

In this work, a methodology was developed to model the entire fuel injection system from the pump to the catch tank at the end of the return line, including the fuel piping, a shutdown and safety valve, and the injectors. The model was then used to investigate and optimize the system architecture numerically, from the insertion of a resonator at the pump outlet to the sensitivity analysis of the piping length depending on the system placement on the ship. This methodology was applied to a retrofit engine under development at Wärtsilä and later validated via correlation against measurements acquired on a prototype engine at the test bench. Results demonstrated that virtualization of the design process through multi-physics simulation is a powerful means to speed up product development and system integration.

1 INTRODUCTION

The maritime industry is at a pivotal point as it strives to minimize its environmental impact and comply with increasingly stringent emissions regulations. Research and development efforts have demonstrated that methanol is a promising alternative fuel for internal combustion engines (ICEs) in naval applications, offering a potential pathway toward carbon-neutral or even carbon-negative marine operations [1][2][3].

Although methanol has been considered and used as a marine fuel for several years, its adoption has gained significant momentum in the past decade, driven by the need for more sustainable fuel options and compliance with stricter emissions standards [4][5].

Implementing methanol as a marine fuel requires compliance with international regulations, such as those set by the International Maritime Organization (IMO). These regulations encompass safety standards and emission limits, critical for the widespread adoption of alternative fuel in the maritime industry [6][7].

When it comes to potential benefits, the usage of methanol includes the reduction of sulfur oxides (SO_x), nitrogen oxides (NO_x), and particulate matter emissions compared to conventional marine fuels [8].

Additionally, the possibility of producing methanol from renewable sources further enhances its potential to lower the carbon footprint of maritime operations [9][1].

Methanol's physical properties, being liquid at ambient temperature and pressure, make it an attractive solution that is easier to store and handle compared to gaseous fuels such as liquefied natural gas (LNG) [10][11].

However, transitioning to methanol as a marine fuel requires modifications to existing engines, including careful engine design, material selection, fuel system management, and the addition of methanol-specific components to ensure safe operation [12][13].

Notably, methanol's corrosiveness, toxicity, and low lubricity present significant hurdles that must be addressed to ensure safe and efficient engine operation [14].

Additionally, methanol's lower energy density than conventional marine fuels may impact fuel storage requirements and overall vessel range. Higher heat of vaporization and lower vapor pressure also need to be managed to avoid cold start issues. Furthermore, high solubility in water can lead to contamination issues, requiring careful management of fuel storage and handling [4][15].

To address these and other technical challenges, numerical simulations have been recognized as a powerful tool for system optimization by allowing investigation and refinement of design parameters in a virtual environment before physical implementation.

This approach significantly accelerates time to market and reduces costs by minimizing the need for extensive prototyping and experimental measurements. Specifically, 1D multi-physics modeling with GT-SUITE has been used to investigate fuel injection system performance and behavior, allowing potential issues to be identified and addressed early in the development process and enabling better management of customer needs by allowing tailored solutions to be tested and validated virtually before deployment.

This paper explores a methodology developed to model and optimize the entire fuel injection system, from the pump to the catch tank at the end of the return line. The simulation setup included the fuel piping, a shutdown and safety valve, and the injectors. The simulation aimed to analyze the behavior and stability of the fuel injection system under various operating conditions with methanol as the primary fuel.

A key aspect of this analysis involved placing a resonator at the pump outlet to dampen pressure oscillations and improve injection stability. Additionally, a sensitivity analysis was conducted to determine the optimal configuration for consistent fuel delivery and system steadiness across different ship placements.

The methodology was applied to a retrofit engine under development at Wärtsilä and validated through correlation with measurements from a prototype engine at the test bench.

2 FUEL SYSTEM MODEL BUILDING

The system studied comprises a methanol circuit coupled with a control oil circuit. The system architecture is reported in Figure 1.

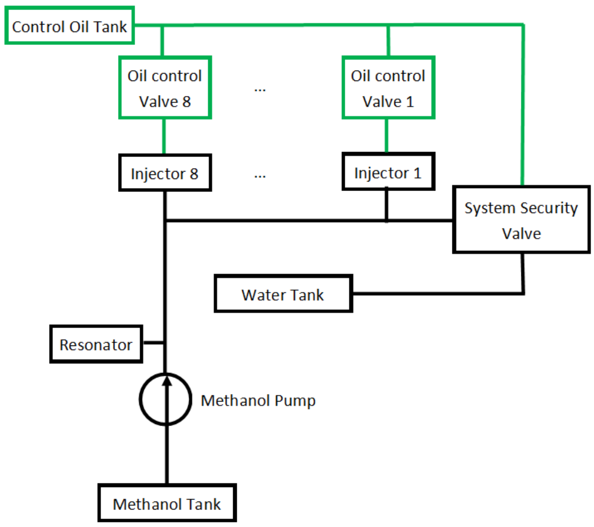

Figure 1. System Architecture

The fuel system model building will be described in the following sections. For each component, the hypothesis considered to reach the best compromise between computational time and accuracy will be detailed [18].

2.1 Main Pump

The main pump is modeled with a dedicated template *PumpFlow* within the GT-SUITE library. In this template, the pump flow is imposed as well as the total isentropic efficiency. This setup enables the definition of the pump flow based on component characterization while also predicting power consumption.

To obtain a higher accuracy, the pump flow pulsations were inserted at several pump speeds. Based on the actual pump speed (either imposed by the user or controlled by a PID controller to reach the target rail pressure), the model will interpolate to impose the corresponding flow pulsations vs. pump angle.

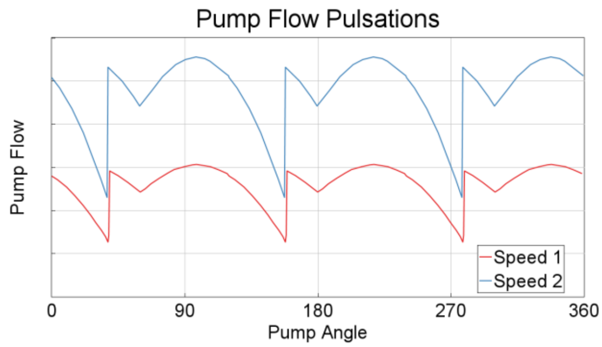

Figure 2. Fuel Pump Input Data

Potentially, these curves can be updated by the user to represent various configurations (e.g., pump used on the ship vs. pump used on the test bench).

2.2 Piping

To build a model that closely represents the actual geometry, the methodology starts from the CAD system. An example is reported in Figure *3*.

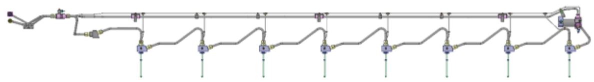

Figure 3. Piping Input CAD

Starting from this CAD, the first step is to extract the wetted surface. The CAD displayed in Figure *3* is, at the end of this step, post-processed into the geometry displayed in Figure *4* where the piping can be clearly identified as well as some T-junctions splitting the flow between the various branches (e.g. various cylinders).

Figure 4. Extracted Volume

Then, through dedicated tools within GEM-3D, each pipe is converted into a dedicated *Pipe* template, automatically extracting the required inputs (diameter, length, eventual radius of curvature, and angle...). The volumes splitting the fuel into several paths are converted into *Flowsplit* object allowing to predict, thanks to simplified 1D hypothesis, the pressure pulsations propagation and the flow distribution. The circuit is then exported into GT-ISE to be integrated with the model of each component. The exported model representing the piping of interest is reported in Figure *5*.

Figure 5. GT-SUITE Piping Model

2.3 Injector

The injector inserted in the circuit of interest is designed in collaboration with OMT (Officine Meccaniche Torino Spa), a Wärtsilä supplier. A detailed GT-SUITE model of the component was built by OMT, able to predict the needle lift and associated instantaneous methanol mass flow based on geometrical inputs. The model was correlated with experimental measurements from a standalone injector test bench.

The correlation obtained in terms of cumulative injected mass is reported in Figure *6*, with the simulated results displayed in red and the experimental measurement in black dashed line.

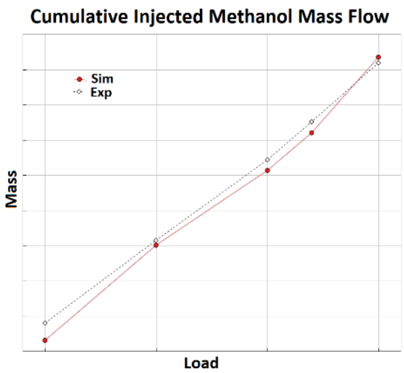

Figure 6. Injector Standalone Model Correlation

Based on the good level of correlation observed, the built model was integrated into the complete fuel circuit as a black-box model. This sub-model features four ports

- Fuel Inlet Flow Port
- Oil Inlet Flow Port for actuation
- Oil Inlet Flow Port for sealing
- Oil Outlet leakage port

Moreover, the user can update the nozzle geometry (number of holes and diameter of the single hole) as well as the cylinder pressure.

2.4 Oil Control Valve

The injector needle displacement is controlled by the oil pressure in the control chamber above the needle itself, thanks to an electronic valve.

In particular, a 3/2 DCV oil control valve, as described in Figure 7 is installed upstream of the injectors' oil ports. It features three ports connected to the oil circuit as follows:

- The port A connected to the oil pressurized port
- The port P connected to the piping leading to the injector control chamber
- The port T connected to the oil tank at design pressure.

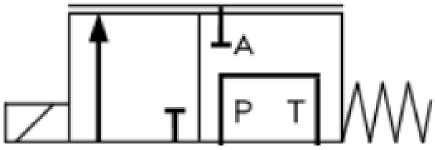

Figure 7. Oil Control Valve Configuration

Without electronic actuation the port A is capped while the port P is connected to the port T. With actuation, the spool shifts to its second contact position allowing a connection between the A and P ports while capping the tank port.

Such a valve is modeled in GT-SUITE with a chamber connected directly to the port P. Two orifices whose opening is externally actuated are connecting this chamber with the two remaining ports (A and T). The pressure drop through each of these connections when fully open is imposed as well as the curves of opening area as a function of the valve lift, as shown in Figure *8*.

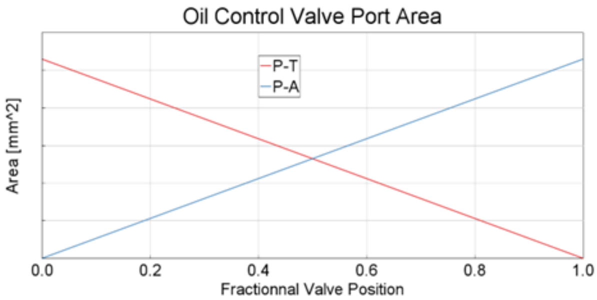

Figure 8. Oil Control Valve Opening Area

The electrical actuation current is imposed with a parametric profile as reported in Figure *9*.

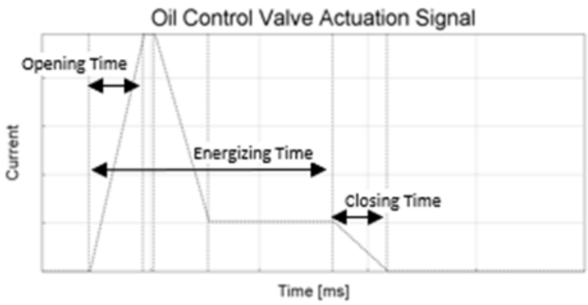

Figure 9. Oil Control Valve Actuation Signal

To sum up, a scheme of the Oil Control Valve GT-SUITE model converting the actuation signal into a port area is reported in Figure *10*.

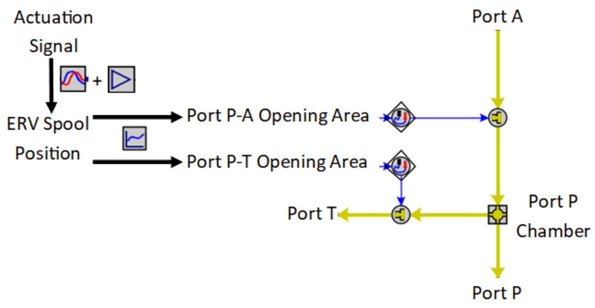

Figure 10. Scheme Oil control valve Model

The built model allows to predict the interactions between the control signal and the pressure pulsations. An example is shown in Figure 11 where the drop of pressure in port A and the increase of pressure in port P is predicted, caused by the P-A port opening. This delay between the port opening and the electrical signal rise is caused by some mechanical delay, such as the spool inertia, introduced between the electrical signal and the valve spool displacement. At the spool valve closure, a peculiar pressure trend at port P is observed with a drop of pressure followed by a long bump. This phenomenon is caused by the interaction between the Oil control valve and the injector, particularly due to a pressure wave traveling back from the injector to the Oil control valve upon injector closure.

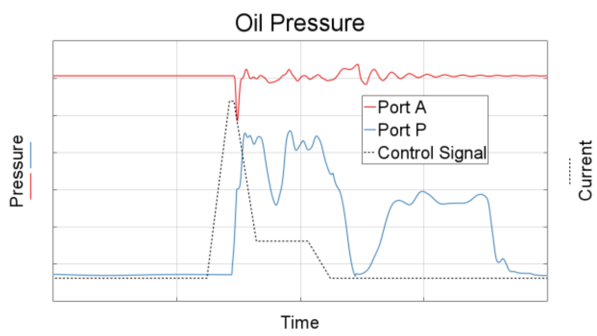

Figure 11. Oil Pressure at valve ports

2.5 Start and Safety Valve (SSV)

The system includes a safety valve located at the end of the rail. When the valve opens, it connects the fuel rail to the purge line, allowing the circuit to be emptied and subsequently purged with nitrogen. This action can be triggered by two mechanisms:

- **Safety Opening**: Triggered when the fuel pressure in the rail exceeds a specified threshold.
- **User Opening**: Activated by opening a solenoid valve within the oil circuit, causing a pressure drop in a chamber that acts on the back of the main internal piston of the SSV, thereby opening the valve on the methanol side.

Overall, the SSV incorporates several masses that, through displacement, open flow channels, enabling fluid movement from the high-pressure rail to the purge line.

To accurately predict the interaction between the fluid and the mechanical components, Fluid-Mechanical Templates (FMT) are available in GT-SUITE. This interaction typically involves the following phenomena:

- **Flow Area Variation:** The valve's flow area changes as the valve lift varies.
- **Flow-Induced Forces:** The flowing fluid exerts forces on the valve masses.
- **Volume Changes:** The flow volume changes as the valve lift varies.

To provide a glimpse of the constructed model, Figure 12 illustrates the first part of the system, featuring a ball valve with a conical seat. The CAD representation is shown on the left, with the corresponding GT-SUITE object on the right. The template is connected on the fluid side to the inlet pipe and the outlet volume (highlighted in orange) and on the mechanical side to a Mass object to account for the ball's inertial effect.

In this system, the ball is positioned between the housing and a ball holder piston. For modeling simplicity, it was assumed that the ball and the ball holder are physically attached (even though this does not represent the actual configuration) to prevent numerical instabilities during valve opening.

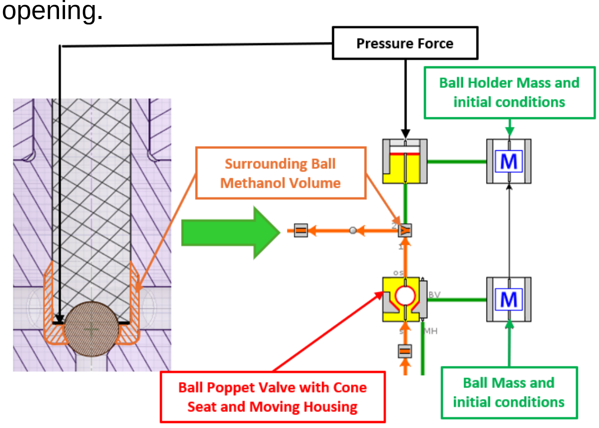

Figure 12. Extract of the Start and Safety Valve Model

The remainder of the system was modeled with the same level of accuracy, enabling precise predictions of system behavior. This approach allowed for simulating not only steady operating points (with the SSV closed) but also dynamic conditions, including system purges.

2.6 Resonator

In some configurations, excessive pulsations are observed at the pump outlet, potentially damaging the piping. A resonator can be installed directly at the main pump outlet to dampen these pulsations. In this project, the geometry of such a resonator is optimized by the pump supplier, taking into account the pump characteristics (number of pistons, expected flow, resonant frequency). A digital twin of this resonator was built in GT-SUITE to evaluate its impact on system performance numerically. Figure 13 shows a detailed view of the resonator's inlet section, with the GT-SUITE model on the right and the CAD representation on the left.

Geometric data for the various internal pipes were incorporated into the model, enabling predictive simulations. This approach is particularly valuable for assessing the resonator’s impact prior to the availability of experimental measurements.

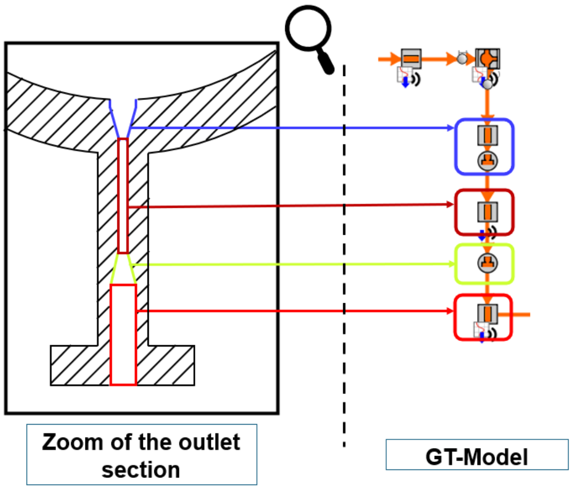

Figure 13. Resonator inlet section model

3 SENSITIVITY ANALYSIS

The built system model described in section 2 was utilized for system design prior to the availability of the first prototype and corresponding experimental measurements.

This model was used as a digital twin to assess the impact of several potential improvements without the need for physical testing. For the sake of brevity, the results of only two of these analyses will be shared:

- **Sensitivity to Resonator Insertion at the Pump Outlet**: Evaluating the effect of adding a resonator at the pump outlet.
- **Sensitivity to Pump Outlet Pipe Geometry**: Considering variations in pump outlet piping, as different configurations are expected between the test rig and the ship.

Among the findings, the relative dispersion of injected fuel quantity was calculated as

$$Dispersion = \frac{Max\ Inj\ Quantity - Min\ Inj\ Quantity}{Total\ Injected\ quantity} * 100$$

3.1 Resonator at Pump Outlet

The resonator model described in Section 2.6 was integrated into the system, and its performance was evaluated at the 100% load operating point. As expected, the resonator demonstrates the greatest impact near the pump outlet and the inlet of the long pipe, which are located close to the resonator. A significant reduction in pressure amplitude is observed in Figure *14*.

Furthermore, the pressure FFT comparison reveals that all frequencies are effectively damped. These results numerically validate the potential benefits of incorporating this component, providing valuable support for the decision-making process.

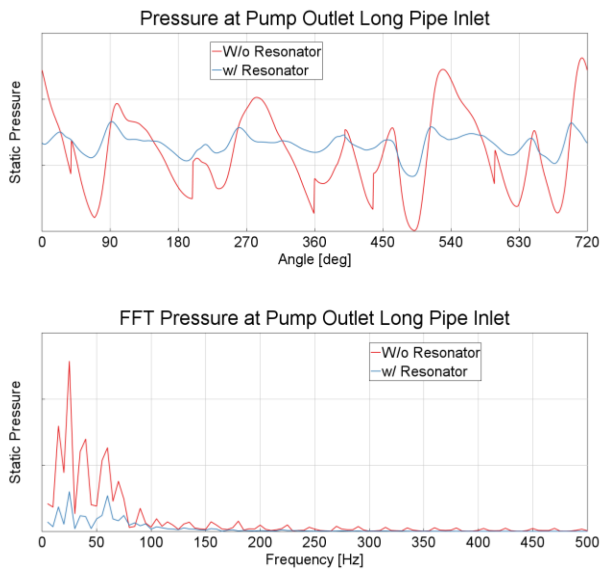

Figure 14. Resonator sensitivity – Pressure trace at Pump Outlet Long Pipe Inlet

Moreover, the pressure amplitudes within the various injector quill pipes were compared by examining the dispersion observed without the resonator (Figure 15) and with the resonator (Figure 16), to check the impact of the resonator further away from its location but on a more critical aspect of the system design.

The results show a similar trend, with the lowest pressure amplitude occurring in the second-to-last injector. The resonator seems to have a reduced impact on cylinder-to-cylinder dispersion, both in terms of pressure amplitude at the quill pipe inlet and in terms of injected quantity, as reported in Figure 17.

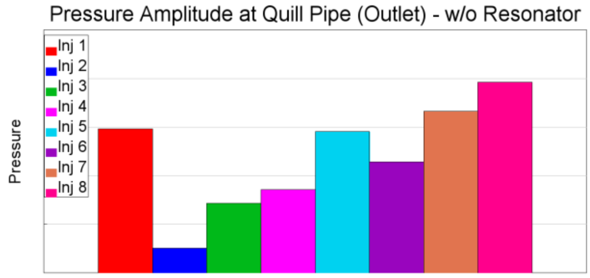

Figure 15. Resonator sensitivity – Pressure Amplitude without resonator

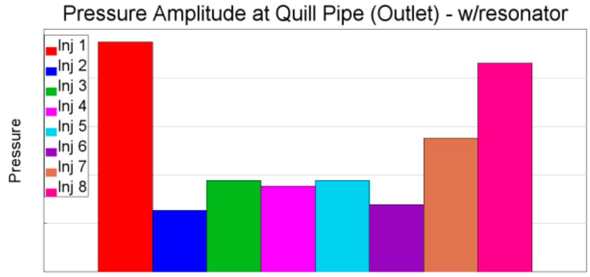

Figure 16. Resonator sensitivity – Pressure Amplitude with resonator

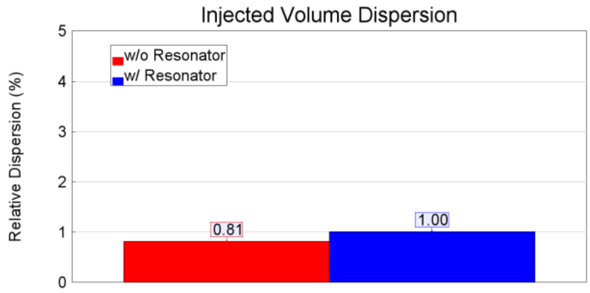

Figure 17. Resonator sensitivity – Injected Volume Dispersion

3.2 Pump Outlet Pipe configuration

As a second sensitivity analysis, two different pipes at the pump outlet were tested, respectively called "Pipe #1" and "Pipe #2". In particular, Pipe #2 is much shorter (38% length reduction) than Pipe #1, but both pipes have the same internal diameter. Moreover, the "Pipe #1" configuration features a flexible hose to connect the pump to the long rigid piping. Instead, in the "Pipe #2" configuration, the long rigid pipe is directly connected to the pump.

First of all, when looking at the pressure at the pump outlet long pipe inlet (Figure *18*), some high differences can be observed. This result can mainly be justified by the flexible hose in the "Pipe #1" configuration, located between the pump and the pump outlet long pipe inlet where the virtual sensor is located. This flexible hose tends to reduce the pressure pulsations amplitude, especially around 70Hz.

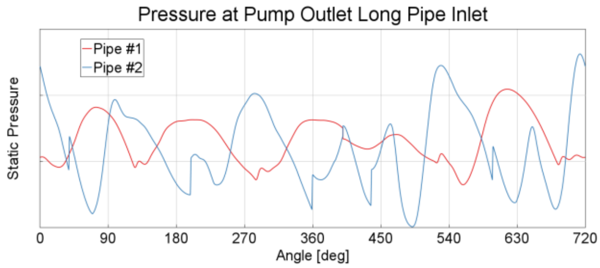

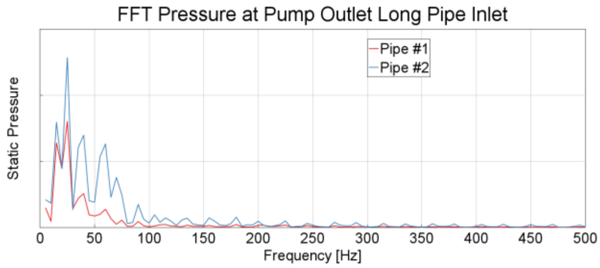

Figure 18. Pump Outlet Pipe sensitivity – Pressure trace at Pump Outlet Long Pipe Inlet

As in the previous section, in Figure 19 and Figure 20 are reported the pressure amplitude dispersion with the two pipe configurations.

In this sensitivity analysis the impact is limited, a slight reduction of 4% of the dispersion (still observed between cylinder 2 and cylinder 8) is noticed. These results could be explained by a higher impact of the injector characteristics and rail geometry on this output while the pump outlet piping has a reduced influence.

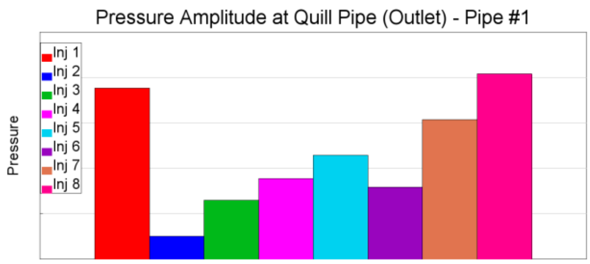

Figure 19. Pump Outlet Pipe sensitivity – Pressure Amplitude with Pipe #1

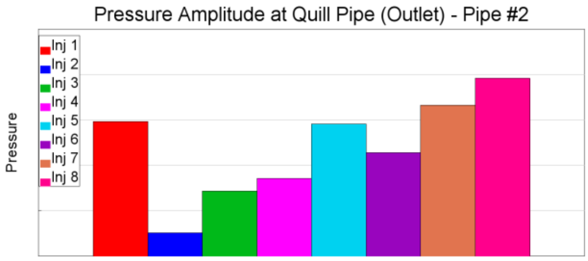

Figure 20. Pump Outlet Pipe sensitivity – Pressure Amplitude with Pipe #2

In terms of injected volume dispersion, again, the change in piping does not change significantly this critical output for the system design. This result was expected, a higher impact would be expected from a change in the piping much closer to the injectors (e.g. rail, quill pipe).

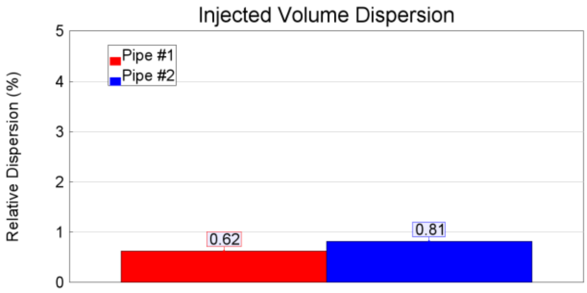

Figure 21. Pump Outlet Pipe sensitivity – Injected Volume Dispersion

4 MODEL VALIDATION

The system was run in the Wärtsilä Trieste laboratory on a W7L46F having a rated power of 1200 kW/cylinder. The system was set up with a methanol high-pressure pump, a high-pressure feed pipe of about 10 meters, and connected to the W46F engine converted for methanol operation. A proper test plan was prepared to map and find the optimal set points in terms of timing and rail pressure at different loads. Once performance optimization was concluded, a simulation was performed with the final parameters in terms of rail pressure and quantity injected at the different loads to compare it with engine measurements. Three sensors have been installed in the system to track the behavior of different parameters on the engine; in particular, the pressure sensors were installed to make a comparison with the simulation.

The three sensors were located, as shown in Figure 22 one at the high-pressure feed pipe inlet, one at the high-pressure feed pipe outlet, and the other in the quill pipe T block of the #3 cylinder.

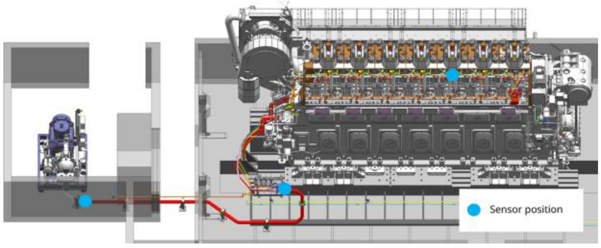

Figure 22. Sensor position

The results at 100% are reported in the next sections as they showed to be representative of the level of correlation observed on a sweep of load from 25% to 100%.

4.1 Sensor in T piece cylinder #3

The initial focus was on evaluating the sensor in cylinder #3 to ensure that the pressure pulsations generated by the engine were accurately represented in the simulation. As shown in Figure 23, the simulation closely aligns with the experimental measurements in terms of the pressure pulsation waveform, with minor deviations observed in amplitude. Additionally, the FFT analysis of the pressure traces demonstrates a strong agreement between the simulation and experimental data. In particular the first peak at 30Hz is well reproduced. Instead, the second peak at 60Hz is underestimated.

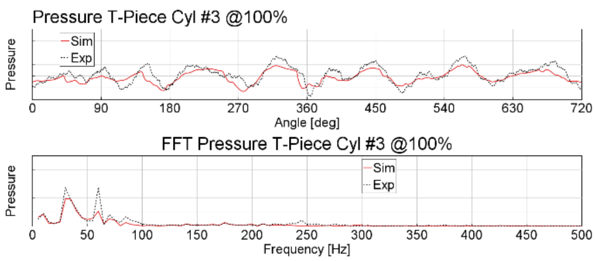

Figure 23. Correlation Pressure T-Piece Cylinder #3 at 100% Load

4.2 Sensor at inlet of the High-pressure Feed pipe

An evaluation of the high-pressure feed pipe pressure sensors was conducted. Figure 24 Presents a comparison between the simulation and the experimental measurements at the pipe inlet. While the general trend is captured, discrepancies are observed in the alignment of peaks and amplitude. However, looking at the frequency content, the match is well aligned, particularly at the lowest frequencies. Some higher amplitudes around 100Hz, not observed downstream in the fuel line, are not predicted. However, it should be highlighted that the GT-SUITE model was not tuned. An improvement can be expected with further analysis and model-tuning effort.

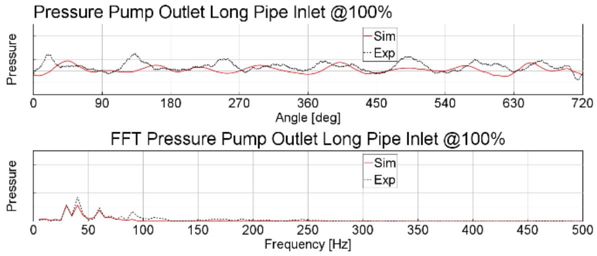

Figure 24. Correlation Pressure Pump Outlet Long Pipe Inlet at 100% Load

4.3 Sensor at outlet of the High-pressure Feed pipe

Finally, experimental and simulation results were compared for the sensor located at the High-pressure pipe outlet. The FFT result shows a good match between the simulation and experimental results in terms of main frequencies, while the simulation underestimates the amplitude of the pressure, particularly at 40Hz and 90Hz. Instead, looking at the instantaneous pressure traces, the mismatch is more pronounced, probably due to a difference in the phasing of the waves.

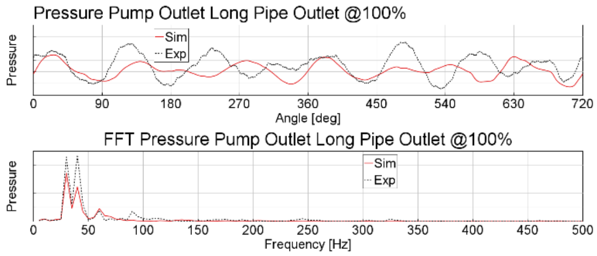

Figure 25. Correlation Pressure Pump Outlet Long Pipe Outlet at 100% Load

4.4 General considerations

Although the model did not undergo a structured and formal calibration process but relied primarily on initial expert judgment, it demonstrated reliability and facilitated progress in design activities. As a result, it enabled the development of components that met all performance goals, which were successfully validated through testing. This achievement highlights the model's effectiveness, and further development is expected to enhance its overall performance and accuracy

5 CONCLUSIONS

A comprehensive methodology was developed to construct a digital twin of the methanol injection circuit currently under development. Key components, including the high-pressure pump, injector, and safety features such as the Start and Safety Valve, were modeled with detail that effectively balances computational efficiency and accuracy.

The robustness and fidelity of the constructed model enabled virtual calibration activities, such as evaluating the impact of a resonator at the pump outlet on critical system design factors. These simulations provided valuable insights that helped the system's development process.

Subsequently, the model was validated against data from the first prototypes. While some discrepancies were observed in the amplitude of pressure oscillations, the model successfully predicted key trends, such as the influence of engine load, and accurately captured the frequency content of pressure traces without requiring additional model tuning. These results confirm the validity and reliability of the proposed methodology, demonstrating its applicability for advancing the design and optimization of methanol injection systems.

6 DEFINITIONS, ACRONYMS, ABBREVIATIONS

DCV: Directional Control Valve

SSV: Start and Safety Valve

FFT: Fast Fourier Transform

FMT: Fluid-Mechanical Templates

7 REFERENCES AND BIBLIOGRAPHY

[1] Su, G., Zulkifli, N. W. M., Liu, L., Ong, H. C., Ibrahim, S., Yu, K. L., Wei, Y., & Bin, F. 2023. Carbon-negative co-production of methanol and activated carbon from bagasse pyrolysis, physical activation, chemical looping, and methanol synthesis. *Energy Conversion and Management*, 293.

[2] Lindstad, E., Lagemann, B., Rialland, A., Gamlem, G. M., & Valland, A. 2021. Reduction of maritime GHG emissions and the potential role of E-fuels. Transportation Research Part D: *Transport and Environment*, 101.

[3] Parris, D., Spinthiropoulos, K., Ragazou, K., Giovou, A., & Tsanaktsidis, C. 2024. Methanol, a Plugin Marine Fuel for Green House Gas Reduction,A Review. *Energies*, 17(3), 605.

[4] Korberg, A. D., Brynolf, S., Grahn, M., & Skov, I. R. 2021. Techno-economic assessment of advanced fuels and propulsion systems in future fossil-free ships. *Renewable and Sustainable Energy Reviews*, 142.

[5] Xing, H., Stuart, C., Spence, S., & Chen, H. 2021. Alternative fuel options for low carbon maritime transportation: Pathways to 2050. *Journal of Cleaner Production*, 297.

[6] Olmer, N., Comer, B., Roy, B., Mao, X., & Rutherford, D. 2017. Greenhouse Gas Emissions from Global Shipping, 2013-2015. *The International Council on Clean Transportation*.

[7] IMO 2020. Cleaner shipping for cleaner air. International Maritime Organization Regulations. Retrieved from https://www.imo.org

[8] Brynolf, S., Fridell, E., & Andersson, K. 2014. Environmental Assessment of Marine Fuels: Liquefied Natural Gas, Liquefied Biogas, Methanol, and Bio-Methanol. *Journal of Cleaner Production*, 74, 86-95.

[9] Balcombe, P., Brierley, J., Lewis, C., Skatvedt, L., Speirs, J., Hawkes, A., & Staffell, I. 2020. How to Decarbonise International Shipping: Options for Fuels, Technologies and Policies. *Energy Conversion and Management*, 182, 72-88.

[10] SGS-INSPIRE-Methanol-Properties-and-Uses, 2020. Methanol Institute. *Retrieved from https://www.methanol.org*

[11] Brynolf, S., Fridell, E., & Andersson, K. 2014. Environmental assessment of marine fuels: liquefied natural gas, liquefied biogas, methanol and bio-methanol. *Journal of Cleaner Production,* 74, 86-95.

[12] Hansson, J., Brynolf, S., Fridell, E., & Lehtveer, M. 2020. The Potential Role of Ammonia as Marine Fuel—Based on Energy Systems Modeling and Multi-Criteria Decision Analysis. *Sustainability*, 12(8), 3265.

[13] Wärtsilä. 2019. Methanol as a Marine Fuel: Technical and Operational Considerations. Wärtsilä Corporation.

[14] Lindstad, H., & Eskeland, G. S. 2016. Environmental Regulations in Shipping: Policies and Compliance. *Transportation Research Part D: Transport and Environment,* 47, 1-6.

[15] Bilgili, L. ,2021. Comparative assessment of alternative marine fuels in life cycle perspective. *Renewable and Sustainable Energy Reviews*, 144.

[16] Verhelst S., Turner J.WG , Vancoillie Louis .S., J.2019, Methanol as a fuel for internal combustion engines, *Progress in Energy and Combustion Science*, Volume 70.

[17] Onorati A., Montenegro G.2020,*1D and Multi-D Modeling Techniques for IC Engine Simulation*, SAE International, Warrendale, Pennsylvania, USA

[18] Gamma Technologies LLC, “*GT-SUITE User's Manual*”, 2024.